

Neural Networks for Analysis of Top Quark Production

The DØ Collaboration *

Fermi National Accelerator Laboratory, Batavia, Illinois, 60510

(July 15, 1999)

Abstract

Neural networks (NNs) provide a powerful and flexible tool for selecting a signal from a larger background. The DØ collaboration has used them extensively in studying $t\bar{t}$ decays. NNs were essential to the measurement of the $t\bar{t}$ production cross section in the all-jets channel ($t\bar{t} \rightarrow b\bar{b}qqqq$), and were also used in the measurement of the mass of the top quark in the lepton+jets channel ($t\bar{t} \rightarrow b\bar{b}l\nu q\bar{q}$). This paper will describe two new applications of neural networks to top quark analysis: the search for single top quark production, and an effort to increase the sensitivity in the dilepton channel $t\bar{t} \rightarrow b\bar{b}e\bar{\mu}\nu\bar{\nu}$ beyond that achieved in the published analysis.

arXiv:hep-ex/9907041v1 21 Jul 1999

*Submitted to the *International Europhysics Conference on High Energy Physics, EPS-HEP99*, 15–21 July, 1999, Tampere, Finland.

B. Abbott,⁴⁵ M. Abolins,⁴² V. Abramov,¹⁸ B.S. Acharya,¹¹ I. Adam,⁴⁴ D.L. Adams,⁵⁴ M. Adams,²⁸ S. Ahn,²⁷ V. Akimov,¹⁶ G.A. Alves,² N. Amos,⁴¹ E.W. Anderson,³⁴ M.M. Baarmand,⁴⁷ V.V. Babintsev,¹⁸ L. Babukhadia,²⁰ A. Baden,³⁸ B. Baldin,²⁷ S. Banerjee,¹¹ J. Bantly,⁵¹ E. Barberis,²¹ P. Baringer,³⁵ J.F. Bartlett,²⁷ A. Belyaev,¹⁷ S.B. Beri,⁹ I. Bertram,¹⁹ V.A. Bezzubov,¹⁸ P.C. Bhat,²⁷ V. Bhatnagar,⁹ M. Bhattacharjee,⁴⁷ G. Blazey,²⁹ S. Blessing,²⁵ P. Bloom,²² A. Boehnlein,²⁷ N.I. Bojko,¹⁸ F. Borcharding,²⁷ C. Boswell,²⁴ A. Brandt,²⁷ R. Breedon,²² G. Briskin,⁵¹ R. Brock,⁴² A. Bross,²⁷ D. Buchholz,³⁰ V.S. Burtovoi,¹⁸ J.M. Butler,³⁹ W. Carvalho,² D. Casey,⁴² Z. Casilum,⁴⁷ H. Castilla-Valdez,¹⁴ D. Chakraborty,⁴⁷ S.V. Chekulaev,¹⁸ W. Chen,⁴⁷ S. Choi,¹³ S. Chopra,²⁵ B.C. Choudhary,²⁴ J.H. Christenson,²⁷ M. Chung,²⁸ D. Claes,⁴³ A.R. Clark,²¹ W.G. Cobau,³⁸ J. Cochran,²⁴ L. Coney,³² W.E. Cooper,²⁷ D. Coppage,³⁵ C. Cretsinger,⁴⁶ D. Cullen-Vidal,⁵¹ M.A.C. Cummings,²⁹ D. Cutts,⁵¹ O.I. Dahl,²¹ K. Davis,²⁰ K. De,⁵² K. Del Signore,⁴¹ M. Demarteau,²⁷ D. Denisov,²⁷ S.P. Denisov,¹⁸ H.T. Diehl,²⁷ M. Diesburg,²⁷ G. Di Loreto,⁴² P. Draper,⁵² Y. Ducros,⁸ L.V. Dudko,¹⁷ S.R. Dugad,¹¹ A. Dyshkant,¹⁸ D. Edmunds,⁴² J. Ellison,²⁴ V.D. Elvira,⁴⁷ R. Engelmann,⁴⁷ S. Eno,³⁸ G. Eppley,⁵⁴ P. Ermolov,¹⁷ O.V. Eroshin,¹⁸ H. Evans,⁴⁴ V.N. Evdokimov,¹⁸ T. Fahland,²³ M.K. Fatyga,⁴⁶ S. Feher,²⁷ D. Fein,²⁰ T. Ferbel,⁴⁶ H.E. Fisk,²⁷ Y. Fisyak,⁴⁸ E. Flattum,²⁷ G.E. Forden,²⁰ M. Fortner,²⁹ K.C. Frame,⁴² S. Fuess,²⁷ E. Gallas,²⁷ A.N. Galyaev,¹⁸ P. Garton,²⁴ V. Gavrilov,¹⁶ T.L. Geld,⁴² R.J. Genik II,⁴² K. Genser,²⁷ C.E. Gerber,²⁷ Y. Gershtein,⁵¹ B. Gibbard,⁴⁸ B. Gobbi,³⁰ B. Gómez,⁵ G. Gómez,³⁸ P.I. Goncharov,¹⁸ J.L. González Solís,¹⁴ H. Gordon,⁴⁸ L.T. Goss,⁵³ K. Gounder,²⁴ A. Goussiou,⁴⁷ N. Graf,⁴⁸ P.D. Grannis,⁴⁷ D.R. Green,²⁷ J.A. Green,³⁴ H. Greenlee,²⁷ S. Grinstein,¹ P. Grudberg,²¹ S. Grünendahl,²⁷ G. Guglielmo,⁵⁰ J.A. Guida,²⁰ J.M. Guida,⁵¹ A. Gupta,¹¹ S.N. Gurzhiev,¹⁸ G. Gutierrez,²⁷ P. Gutierrez,⁵⁰ N.J. Hadley,³⁸ H. Haggerty,²⁷ S. Hagopian,²⁵ V. Hagopian,²⁵ K.S. Hahn,⁴⁶ R.E. Hall,²³ P. Hanlet,⁴⁰ S. Hansen,²⁷ J.M. Hauptman,³⁴ C. Hays,⁴⁴ C. Hebert,²⁹ D. Hedin,²⁹ A.P. Heinson,²⁴ U. Heintz,³⁹ R. Hernández-Montoya,¹⁴ T. Heuring,²⁵ R. Hirosky,²⁸ J.D. Hobbs,⁴⁷ B. Hoeneisen,⁶ J.S. Hoftun,⁵¹ F. Hsieh,⁴¹ Tong Hu,³¹ A.S. Ito,²⁷ S.A. Jerger,⁴² R. Jesik,³¹ T. Joffe-Minor,³⁰ K. Johns,²⁰ M. Johnson,²⁷ A. Jonckheere,²⁷ M. Jones,²⁶ H. Jöstlein,²⁷ S.Y. Jun,³⁰ C.K. Jung,⁴⁷ S. Kahn,⁴⁸ D. Karmanov,¹⁷ D. Karmgard,²⁵ R. Kehoe,³² S.K. Kim,¹³ B. Klima,²⁷ C. Klopfenstein,²² B. Knuteson,²¹ W. Ko,²² J.M. Kohli,⁹ D. Koltick,³³ A.V. Kostitskiy,¹⁸ J. Kotcher,⁴⁸ A.V. Kotwal,⁴⁴ A.V. Kozelov,¹⁸ E.A. Kozlovsky,¹⁸ J. Krane,³⁴ M.R. Krishnaswamy,¹¹ S. Krzywdzinski,²⁷ M. Kubantsev,³⁶ S. Kuleshov,¹⁶ Y. Kulik,⁴⁷ S. Kunori,³⁸ F. Landry,⁴² G. Landsberg,⁵¹ A. Leflat,¹⁷ J. Li,⁵² Q.Z. Li,²⁷ J.G.R. Lima,³ D. Lincoln,²⁷ S.L. Linn,²⁵ J. Linnemann,⁴² R. Lipton,²⁷ A. Lucotte,⁴⁷ L. Lueking,²⁷ A.K.A. Maciel,²⁹ R.J. Madaras,²¹ R. Madden,²⁵ L. Magaña-Mendoza,¹⁴ V. Manankov,¹⁷ S. Mani,²² H.S. Mao,⁴ R. Markeloff,²⁹ T. Marshall,³¹ M.I. Martin,²⁷ R.D. Martin,²⁸ K.M. Mauritz,³⁴ B. May,³⁰ A.A. Mayorov,¹⁸ R. McCarthy,⁴⁷ J. McDonald,²⁵ T. McKibben,²⁸ J. McKinley,⁴² T. McMahon,⁴⁹ H.L. Melanson,²⁷ M. Merkin,¹⁷ K.W. Merritt,²⁷ C. Miao,⁵¹ H. Miettinen,⁵⁴ A. Mincer,⁴⁵ C.S. Mishra,²⁷ N. Mokhov,²⁷ N.K. Mondal,¹¹ H.E. Montgomery,²⁷ M. Mostafa,¹ H. da Motta,² C. Murphy,²⁸ F. Nang,²⁰ M. Narain,³⁹ V.S. Narasimham,¹¹ A. Narayanan,²⁰ H.A. Neal,⁴¹ J.P. Negret,⁵ P. Nemethy,⁴⁵ D. Norman,⁵³ L. Oesch,⁴¹ V. Oguri,³ N. Oshima,²⁷ D. Owen,⁴² P. Padley,⁵⁴ A. Para,²⁷ N. Parashar,⁴⁰ Y.M. Park,¹² R. Partridge,⁵¹ N. Parua,⁷ M. Paterno,⁴⁶ B. Pawlik,¹⁵ J. Perkins,⁵² M. Peters,²⁶ R. Piegaiia,¹ H. Piekarz,²⁵ Y. Pischalnikov,³³ B.G. Pope,⁴² H.B. Prosper,²⁵ S. Protopopescu,⁴⁸ J. Qian,⁴¹ P.Z. Quintas,²⁷ R. Raja,²⁷ S. Rajagopalan,⁴⁸ O. Ramirez,²⁸ N.W. Reay,³⁶ S. Reucroft,⁴⁰ M. Rijssenbeek,⁴⁷ T. Rockwell,⁴² M. Roco,²⁷ P. Rubinov,³⁰ R. Ruchti,³² J. Rutherford,²⁰ A. Sánchez-Hernández,¹⁴ A. Santoro,² L. Sawyer,³⁷ R.D. Schamberger,⁴⁷ H. Schellman,³⁰ J. Sculli,⁴⁵ E. Shabalina,¹⁷ C. Shaffer,²⁵ H.C. Shankar,¹¹ R.K. Shivpuri,¹⁰ D. Shpakov,⁴⁷ M. Shupe,²⁰ R.A. Sidwell,³⁶ H. Singh,²⁴ J.B. Singh,⁹ V. Sirotenko,²⁹ E. Smith,⁵⁰ R.P. Smith,²⁷ R. Snihur,³⁰ G.R. Snow,⁴³ J. Snow,⁴⁹ S. Snyder,⁴⁸ J. Solomon,²⁸ M. Sosebee,⁵² N. Sotnikova,¹⁷ M. Souza,² N.R. Stanton,³⁶ G. Steinbrück,⁵⁰ R.W. Stephens,⁵² M.L. Stevenson,²¹ F. Stichelbaut,⁴⁸ D. Stoker,²³ V. Stolin,¹⁶ D.A. Stoyanova,¹⁸ M. Strauss,⁵⁰ K. Streets,⁴⁵ M. Strovink,²¹ A. Sznajder,² P. Tamburello,³⁸ J. Tarazi,²³ M. Tartaglia,²⁷ T.L.T. Thomas,³⁰ J. Thompson,³⁸ D. Toback,³⁸ T.G. Trippe,²¹ P.M. Tuts,⁴⁴ V. Vaniev,¹⁸ N. Varelas,²⁸ E.W. Varnes,²¹ A.A. Volkov,¹⁸ A.P. Vorobiev,¹⁸ H.D. Wahl,²⁵ J. Warchol,³² G. Watts,⁵¹ M. Wayne,³² H. Weerts,⁴² A. White,⁵² J.T. White,⁵³ J.A. Wightman,³⁴ S. Willis,²⁹ S.J. Wimpenny,²⁴ J.V.D. Wirjawan,⁵³ J. Womersley,²⁷ D.R. Wood,⁴⁰ R. Yamada,²⁷ P. Yamin,⁴⁸ T. Yasuda,²⁷ P. Yepes,⁵⁴ K. Yip,²⁷ C. Yoshikawa,²⁶ S. Youssef,²⁵ J. Yu,²⁷ Y. Yu,¹³ Z. Zhou,³⁴ Z.H. Zhu,⁴⁶ M. Zielinski,⁴⁶ D. Zieminska,³¹ A. Zieminski,³¹ V. Zutshi,⁴⁶ E.G. Zverev,¹⁷ and A. Zylberstein⁸

(DØ Collaboration)

¹Universidad de Buenos Aires, Buenos Aires, Argentina

²LAFEX, Centro Brasileiro de Pesquisas Físicas, Rio de Janeiro, Brazil

³Universidade do Estado do Rio de Janeiro, Rio de Janeiro, Brazil

⁴Institute of High Energy Physics, Beijing, People's Republic of China

⁵Universidad de los Andes, Bogotá, Colombia

⁶Universidad San Francisco de Quito, Quito, Ecuador

- ⁷Institut des Sciences Nucléaires, IN2P3-CNRS, Université de Grenoble 1, Grenoble, France
- ⁸DAPNIA/Service de Physique des Particules, CEA, Saclay, France
- ⁹Panjab University, Chandigarh, India
- ¹⁰Delhi University, Delhi, India
- ¹¹Tata Institute of Fundamental Research, Mumbai, India
- ¹²Kyungsoong University, Pusan, Korea
- ¹³Seoul National University, Seoul, Korea
- ¹⁴CINVESTAV, Mexico City, Mexico
- ¹⁵Institute of Nuclear Physics, Kraków, Poland
- ¹⁶Institute for Theoretical and Experimental Physics, Moscow, Russia
- ¹⁷Moscow State University, Moscow, Russia
- ¹⁸Institute for High Energy Physics, Protvino, Russia
- ¹⁹Lancaster University, Lancaster, United Kingdom
- ²⁰University of Arizona, Tucson, Arizona 85721
- ²¹Lawrence Berkeley National Laboratory and University of California, Berkeley, California 94720
- ²²University of California, Davis, California 95616
- ²³University of California, Irvine, California 92697
- ²⁴University of California, Riverside, California 92521
- ²⁵Florida State University, Tallahassee, Florida 32306
- ²⁶University of Hawaii, Honolulu, Hawaii 96822
- ²⁷Fermi National Accelerator Laboratory, Batavia, Illinois 60510
- ²⁸University of Illinois at Chicago, Chicago, Illinois 60607
- ²⁹Northern Illinois University, DeKalb, Illinois 60115
- ³⁰Northwestern University, Evanston, Illinois 60208
- ³¹Indiana University, Bloomington, Indiana 47405
- ³²University of Notre Dame, Notre Dame, Indiana 46556
- ³³Purdue University, West Lafayette, Indiana 47907
- ³⁴Iowa State University, Ames, Iowa 50011
- ³⁵University of Kansas, Lawrence, Kansas 66045
- ³⁶Kansas State University, Manhattan, Kansas 66506
- ³⁷Louisiana Tech University, Ruston, Louisiana 71272
- ³⁸University of Maryland, College Park, Maryland 20742
- ³⁹Boston University, Boston, Massachusetts 02215
- ⁴⁰Northeastern University, Boston, Massachusetts 02115
- ⁴¹University of Michigan, Ann Arbor, Michigan 48109
- ⁴²Michigan State University, East Lansing, Michigan 48824
- ⁴³University of Nebraska, Lincoln, Nebraska 68588
- ⁴⁴Columbia University, New York, New York 10027
- ⁴⁵New York University, New York, New York 10003
- ⁴⁶University of Rochester, Rochester, New York 14627
- ⁴⁷State University of New York, Stony Brook, New York 11794
- ⁴⁸Brookhaven National Laboratory, Upton, New York 11973
- ⁴⁹Langston University, Langston, Oklahoma 73050
- ⁵⁰University of Oklahoma, Norman, Oklahoma 73019
- ⁵¹Brown University, Providence, Rhode Island 02912
- ⁵²University of Texas, Arlington, Texas 76019
- ⁵³Texas A&M University, College Station, Texas 77843
- ⁵⁴Rice University, Houston, Texas 77005

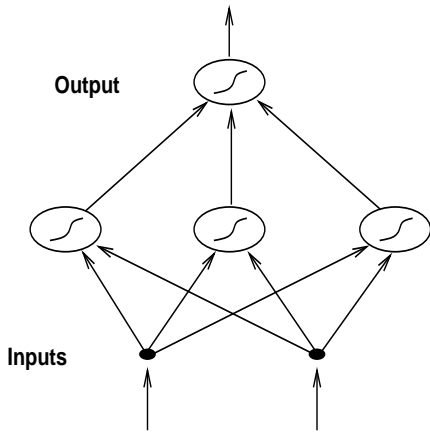


FIG. 1. A feed-forward neural network.

I. INTRODUCTION

Since the observation of the top quark in 1995 [1], much experimental effort has been invested in studying its properties [2]. Such analyses are difficult, owing to the small number of $t\bar{t}$ events available, the relatively large backgrounds, and the complex event geometries. There has therefore been a great deal of interest in analysis techniques that could improve on the standard methods of selecting candidate events. One useful class of such techniques uses pattern classifiers based on feed-forward “neural networks.” [3]

The $D\bar{O}$ experiment at the Fermilab Tevatron has made considerable use of neural network techniques in its analyses of top quark data. Both the cross section measurement in the all-jets channel [4] and the mass measurement in the lepton + jets channel [5] used neural networks; details of these analyses have already been published.

Here, we describe two more recent studies: a neural network analysis of single top quark production, and an effort to improve the efficiency for selecting $t\bar{t} \rightarrow e\mu$ events using neural networks. We shall start with a brief description of the kind of neural networks used in these analyses.

II. NEURAL NETWORKS

Figure 1 shows an example of the type of neural network used in these studies. It consists of a set of processing units, each of which has at least one input and one output. The output y_i of a single unit i is given in terms of its inputs x_{ij} by

$$y_i = g\left(\sum_j x_{ij} + \theta_i\right), \quad (1)$$

where θ_i is a threshold specific to the unit, and g is a nonlinear squashing function, typically of the form

$$g(x) = \frac{1}{1 + e^{-2x}}. \quad (2)$$

[Thus, the unit outputs are bounded in the range $(0, 1)$.] The units are arranged in layers, with the inputs of layer $n + 1$ connected to the outputs of layer n by a weight matrix:

$$x_{ij}^{n+1} = w_{ij}y_j^n. \quad (3)$$

Typically, the last layer consists of only one unit, and is called the “output” layer; the other layers are called “hidden” layers. Often, the y_i^0 are said to be the outputs of a dummy “input” layer. No processing, however, is done in that “layer.” Such a network is quite flexible; in fact, it has been shown that a network with only one hidden layer can approximate any reasonable (Borel-measurable) function to any required degree of accuracy, provided that sufficient units are available in the hidden layer [6].

For pattern recognition, one wants to have the network output 1 if the input is most consistent with signal, and 0 if the input is most consistent with background. Typically, one has available a collection of N inputs, some of which are known to be signal and some of which are known to be background. One defines an error function:

$$\chi^2 = \frac{1}{N} \sum_{i=1}^N (O_i - t_i)^2, \quad (4)$$

where O_i is the output of the network for input i , and t_i is the desired output for that input. This quantity can be considered as a function of the weights \mathbf{w} and thresholds $\boldsymbol{\theta}$; one then minimizes χ^2 with respect to these variables to achieve an approximation to the desired function.

The minimization technique most often used is called “backpropagation,” which is a sort of stochastic gradient descent. Other minimization algorithms can also be used. This process is often referred to as “training” the network.

III. SINGLE TOP QUARK PRODUCTION

The first study we will examine is a search for single top quark production [7]. The processes relevant at the Tevatron are illustrated in Fig. 2; the total cross sections for these processes calculated at next-to-leading order (NLO) are [8]:

$$\begin{aligned} \sigma_{\text{NLO}}(p\bar{p} \rightarrow t\bar{b}X + \text{c.c.}) &= 0.724 \pm 0.043 \text{ pb}, \\ \sigma_{\text{NLO}}(p\bar{p} \rightarrow tq\bar{b}X + \text{c.c.}) &= 1.70 \pm 0.27 \text{ pb}. \end{aligned} \quad (5)$$

Such processes are interesting because they directly probe the $W - t - b$ vertex. Assuming the Standard Model, measuring these cross sections gives a measurement of the V_{tb} element of the Cabibbo-Kobayashi-Maskawa (CKM) matrix. Such measurements are also

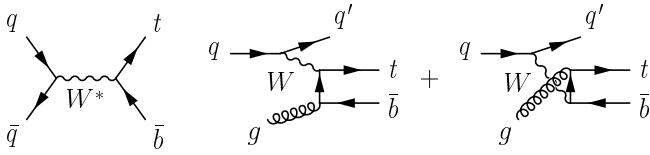


FIG. 2. Feynman diagrams for single top quark production.

sensitive to any new physics in the weak interactions of the top quark [9].

After the decay of the top quark, the particles produced in these processes are $Wb\bar{b}$ and $Wb\bar{b}q$, possibly with additional jets from QCD radiative effects. This study looks for leptonic decays of the W boson, so the initial event selection requires a high- p_T lepton, large missing transverse energy (\cancel{E}_T), and at least two jets. No b -tag is required in this study, in order to preserve signal efficiency (but if information about a tagging muon is present, it will be used).

The numbers of signal and background events expected to remain after this selection for DØ's Run 1 (109 pb⁻¹) are as follows:

Process	N_{events}
$t\bar{b}$	2.1
$tq\bar{b}$	5.1
QCD multijet	2411
$t\bar{t}$	22.3
$Wb\bar{b}$	11.4
Wjj (c, s)	51.8
Wjj (g, u, d)	1615.7
WW	36.9
WZ	5.3

As can be seen, the background is huge compared to the signal, with the dominant background sources being QCD multijet production (with a jet misidentified as a lepton) and the production of W bosons with associated jets.

A crucial step in a neural network analysis is the selection of the variables used as input to the network. Adding more variables potentially increases the amount of information available to the network, but it also expands the space that must be searched during the minimization, making it more difficult to find a good minimum. In fact, with some procedures, adding variables of marginal utility can degrade the performance of a network. And while neural networks can in principle approximate any reasonable function, in practice complicated mappings may require too many hidden nodes for minimization to be practical.

A useful observation is that the rate for a scattering process is greatest in the regions of phase space near singularities in the corresponding matrix element [10]. If such singularities occur in different places for signal and background, then the dependence on the corresponding variables in which the singularities occur should differ strongly between signal and background. For example, the top quark production diagrams in Fig. 2 have a singu-

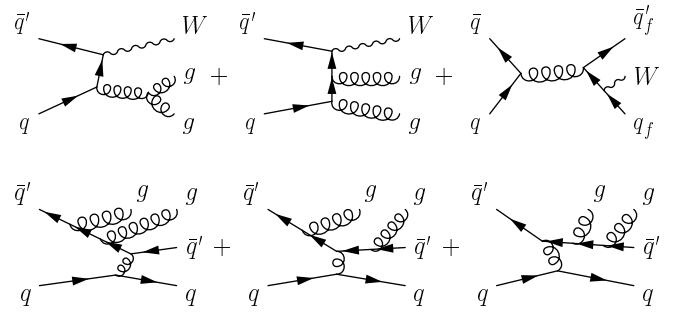


FIG. 3. Typical Feynman diagrams for the Wjj and QCD backgrounds to single top quark production.

larity at $M_t^2 = (p_b + p_W)^2 \rightarrow m_t^2$. In contrast, the dominant background diagrams, illustrated in Fig. 3, have singularities at

$$M_{g1,g2}^2 = (p_{g1} + p_{g2})^2 \rightarrow 0, \quad (6)$$

$$\hat{t}_{q,(g1g2)} = (p_{g1} + p_{g2} - p_q)^2 \rightarrow 0, \quad (7)$$

$$\hat{t}_{q,g1} = (p_{g1} - p_q)^2 \rightarrow 0, \quad (8)$$

$$\hat{t}_{q,g2} = (p_{g2} - p_q)^2 \rightarrow 0. \quad (9)$$

These variables, however, are defined at the parton level, and cannot be directly measured, due to effects of QCD radiation, the unobserved neutrino, and unobserved momentum that escapes down the beam pipe. In such a situation, it is better to use other variables that are related to the singular variables, but can be derived directly from the observed final state. For example, the typical t -channel singular variable $\hat{t}_{i,f}$ associated with the production of a light particle (or jet) f can be written

$$\hat{t}_{i,f} = (p_f - p_i)^2 = -\sqrt{\hat{s}} e^Y p_T^f e^{-|y_f|}, \quad (10)$$

where $\sqrt{\hat{s}}$ is the total invariant mass of the produced system, Y is its total rapidity, and p_T^f and y_f are the transverse momentum and rapidity of the produced f .

From these kinds of considerations, a nominal set of input variables can be defined as:

$$\text{Set 1: } M_{j1,j2}, M_t, Y_{\text{tot}}, p_{Tj1}, y_{j1}, \quad (11)$$

$$p_{Tj2}, y_{j2}, p_{Tj12}, y_{j12}, \sqrt{\hat{s}},$$

where p_{Tj12} and y_{j12} are the transverse momentum and rapidity of the system formed by the two highest p_T jets, and Y_{tot} is the total rapidity of the center of mass of the initial partons, as reconstructed from the final state. The z -component of the momentum of the W boson is found by enforcing the M_W mass constraint in the leptonic W boson decay. Distributions of some of these variables are shown in Fig. 4.

Figure 5 compares this set with the simpler sets:

$$\text{Set 2: } p_{Tj1}, p_{Tj2}, H_{\text{all}}, H_{T\text{all}}; \quad (12)$$

$$\text{Set 3: } p_{Tj1}, p_{Tj2}, H_{\text{all}}, H_{T\text{all}}, M_t; \quad (13)$$

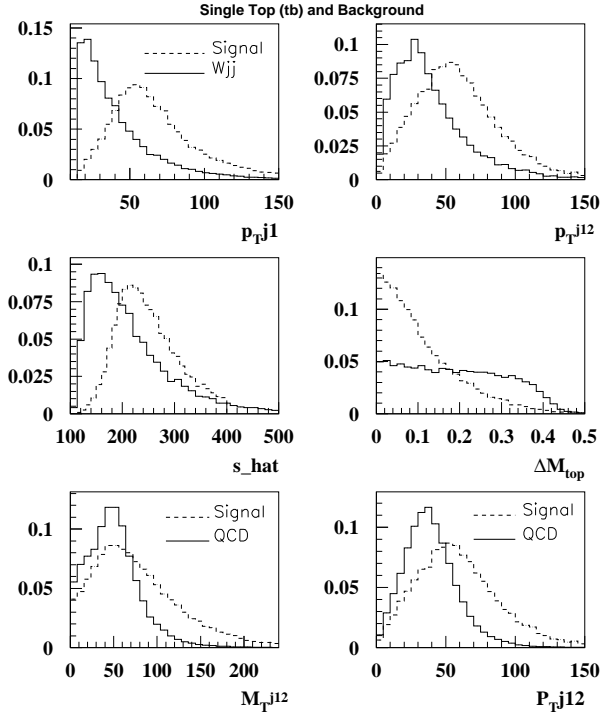


FIG. 4. Distributions of kinematic variables for single top signal (dashed) and background (solid), either Wjj (top four) or QCD (bottom two). Units are in GeV/c^2 .

where $H_{\text{all}} = \sum E_f$ and $H_{T\text{all}} = \sum E_{Tf}$. The comparison is made by training a neural network for each of the sets on a sample of events consisting of top quark signal plus Wjj background. It is seen that the neural network built using Set 1 performs better than those using Set 2 or Set 3.

Figure 5 also shows two other variations of the set of input variables. Set 4 is the same as Set 1, except that the variables H_{all} and $H_{T\text{all}}$ are added. It is seen that this does worse than Set 1 — the additional variables do not add enough information to counteract the increase in the size of the minimization space. Set 5 adds to Set 1 the widths w_{jet} of the two jets and the p_T of a b -tagging muon (set to zero if there is no such tag). In this case, the added variables help: Set 5 has a lower χ^2 than any of the others.

For the final analysis, a separate network is constructed for each of the major backgrounds, as shown in Fig. 6. The networks are trained using JETNET [11]; the results for each network are shown in Fig. 7. Figure 8 shows that the network output from Monte Carlo models agrees well with the data. Finally, individual cuts are made on each of the five network outputs. Figure 9 compares the results of this to a more conventional analysis. It is seen that for a given background level, the neural network analysis provides several times the signal efficiency of conventional cuts.

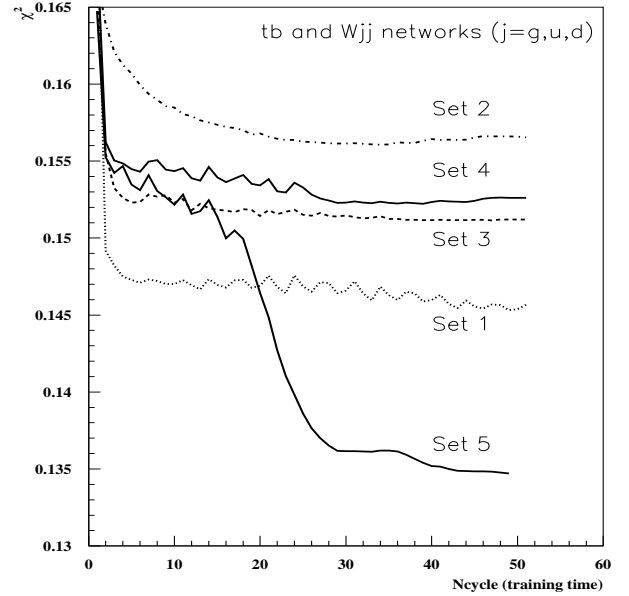


FIG. 5. Neural network χ^2 vs. training time, for different sets of input variables. The networks are trained on a sample consisting of the single top signal and Wjj background.

IV. $t\bar{t}$ DECAYS INTO $e\mu$

The “golden” channel for observing $t\bar{t}$ decays has long been the dilepton mode $t\bar{t} \rightarrow W^+bW^- \bar{b} \rightarrow e\nu_e\mu\nu_\mu\bar{b}\bar{b}$. Due to the presence of two leptons with different flavors, this channel has a very low background. However, compared to the channels in which one of the W bosons decays into jets, the $e\mu$ channel has a relatively small branching ratio — about 2.5%, versus about 15% for the $e + \text{jets}$ channel. Therefore, any new analysis techniques that can increase efficiency for identifying signal in this channel while maintaining the low background level are welcome.

This study starts from the published measurement of the $t\bar{t}$ production cross section [12], which selects $e\mu$ candidates as follows:

- An electron with $E_T > 15$ GeV and $|\eta| < 2.5$.
- A muon with $p_T > 15$ GeV/ c and $|\eta| < 1.2$.
- $\cancel{E}_T > 20$ GeV.
- At least two jets with $E_T > 20$ GeV and $|\eta| < 2.5$.
- $\Delta R_{\mu,\text{jet}} > 0.5$ and $\Delta R_{e,\mu} > 0.25$. ($\Delta R = \sqrt{(\Delta\phi)^2 + (\Delta\eta)^2}$.)
- $H_T > 120$ GeV, where $H_T = E_T^e + \sum_{\text{jets}} E_T^{\text{jet}}$.

For the present study, this selection is relaxed by removing the cut on H_T and reducing the \cancel{E}_T and jet E_T cuts to 15 GeV. This defines the sample used as input to the neural network.

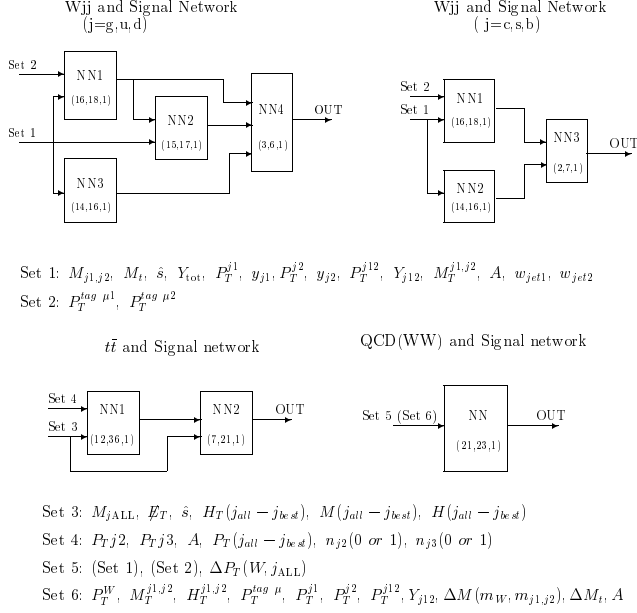


FIG. 6. The structure of the neural networks used to reject each background. Each network has one hidden layer; the notation (n_1, n_2, n_3) gives the number of units in the input, hidden, and output layers of each network, respectively. The following variables are used in addition to those defined in the text. n_{j_2} is 1 if the event has exactly two jets and 0 otherwise; n_{j_3} is 1 if the event has three or more jets and 0 otherwise. The jet for which the invariant mass of the lepton, neutrino, and jet is closest to $172 \text{ GeV}/c^2$ is denoted j_{best} ; the notation $j_{all} - j_{best}$ means all jets except j_{best} . Also, $\Delta P_T(W, j_{all}) = p_T(W) - \sum_{\text{jet}} \vec{p}_T^{\text{jet}}$, $\Delta M(m_W, m_{j_1}, m_{j_2}) = |m_W - m(j_1, j_2)|/m_W$, and $\Delta M_t = |m(e, \nu, j_{best}) - 172|/172$.

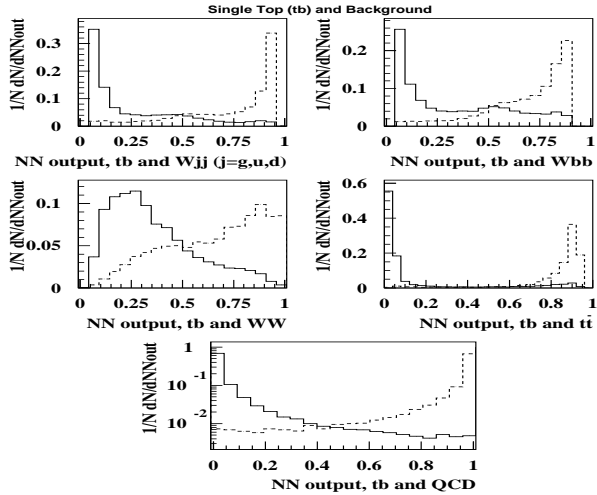


FIG. 7. Outputs of each of the neural networks for single top signal (dashed) and the indicated background (solid).

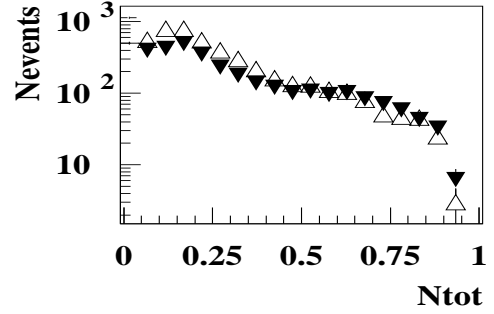


FIG. 8. A comparison of the combined output of the five networks for data (the open symbols) and a Monte Carlo model of signal and all backgrounds (the solid symbols). The individual network outputs are combined using $1/O_{tot} = (1/5) \sum_{i=1}^5 1/O_{NNi}$.

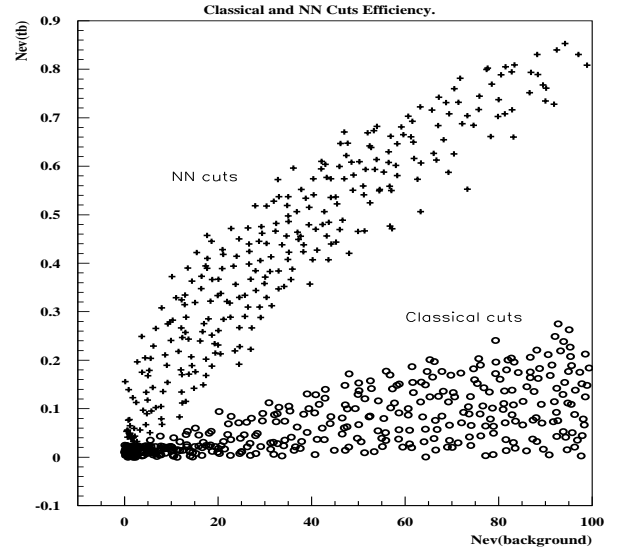


FIG. 9. Comparison of signal/background efficiencies for NN and conventional analyses. Each point represents one specific set of cuts.

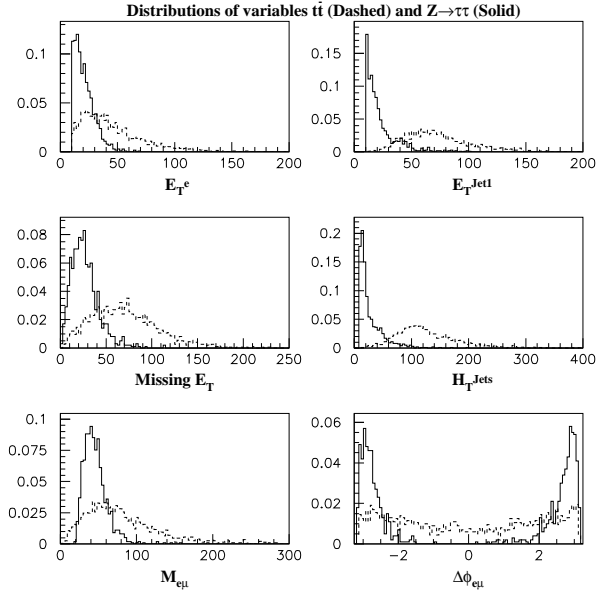


FIG. 10. Distributions of input variables to the $\tau\tau$ neural network for signal (dashed) and $Z \rightarrow \tau\tau$ background (solid).

There are three major backgrounds to contend with: QCD jet production with jets misidentified as leptons, $Z \rightarrow \tau\tau \rightarrow e\mu$, and $WW \rightarrow e\mu$ events. A separate network is trained to separate the signal from each of the three backgrounds. Six variables are used as inputs to each of the networks, these being E_T^e , $E_T^{\text{jet}2}$, \cancel{E}_T , $H_T^{\text{jets}} = \sum_{\text{jets}} E_T^{\text{jet}}$, $M_{e\mu}$, and $\Delta\phi_{e\mu}$, except for the $\tau\tau$ network, where $E_T^{\text{jet}1}$ replaces $E_T^{\text{jet}2}$. The input variables for the $\tau\tau$ network are plotted in Fig. 10. Each network has seven hidden units. The networks are trained (using JETNET) on equal numbers of $t\bar{t}$ signal and background events (2000 of each for the QCD network, and 1000 of each for the other two). The outputs of the three networks are combined, as usual, using

$$O_{\text{NN}}^{\text{comb}} = \frac{3}{\frac{1}{O_{\text{NN}1}} + \frac{1}{O_{\text{NN}2}} + \frac{1}{O_{\text{NN}3}}}. \quad (14)$$

Distributions of this variable for signal and background are shown in Fig. 11. To define the candidate sample, a final cut of $O_{\text{NN}}^{\text{comb}} > 0.88$ is imposed, which was determined by maximizing the expected relative significance, S/σ_B . (σ_B is the uncertainty in the background estimate.)

The resulting signal efficiencies and estimated backgrounds for $D\bar{O}$'s Run 1 (108 pb^{-1}) are shown in Table I and Fig. 12. Compared to the standard (published) analysis, it is seen that the neural network analysis increases the signal efficiency by about 10%. In addition, the background is also slightly lower, although this is harder to evaluate due to the large statistical errors in the QCD background sample. Further comparison is made in Fig. 13.

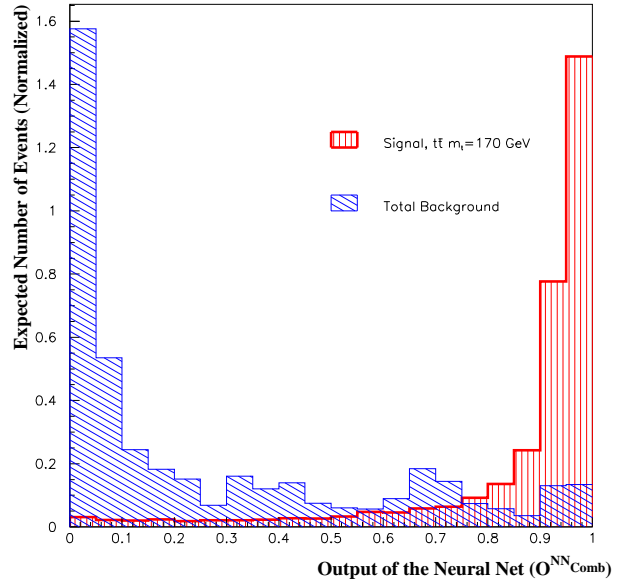


FIG. 11. Distribution of $O_{\text{NN}}^{\text{comb}}$ for $t\bar{t}$ signal and background events.

	Conventional analysis	NN analysis
Signal	$\epsilon \times \text{BR} (\%)$	
$m_t = 170 \text{ GeV}/c^2$	0.349 ± 0.074	0.386 ± 0.082
$m_t = 175 \text{ GeV}/c^2$	0.368 ± 0.078	0.402 ± 0.085
$m_t = 180 \text{ GeV}/c^2$	0.388 ± 0.082	0.420 ± 0.089
Background	N_{expected}	
$Z \rightarrow \tau\tau \rightarrow e\mu$	0.10 ± 0.10	0.10 ± 0.07
$WW \rightarrow e\mu$	0.074 ± 0.020	0.085 ± 0.023
$\gamma^* \rightarrow \tau\tau \rightarrow e\mu$	0.006 ± 0.005	0.007 ± 0.006
Fakes	0.083 ± 0.126	0.048 ± 0.124
Total	0.26 ± 0.16	0.24 ± 0.15

TABLE I. A comparison of the results of the conventional and neural network $t\bar{t} \rightarrow e\mu$ analyses. The numbers of background events are normalized for $D\bar{O}$'s Run 1 (108 pb^{-1}).

V. CONCLUSIONS

In both the analyses considered here, neural networks provide a significant improvement over conventional analysis methods. We expect that such techniques will have a prominent place in the analysis of data from the upcoming Run 2 of the Tevatron.

ACKNOWLEDGMENTS

We thank the Fermilab and collaborating institution staffs for contributions to this work and acknowledge support from the Department of Energy and National Science Foundation (USA), Commissariat à L'Énergie Atomique (France), Ministry for Science and Technology and Ministry for Atomic Energy (Russia), CAPES and CNPq (Brazil), Departments of Atomic Energy and Science and Education (India), Colciencias (Colombia), CONACyT (Mexico), Ministry of Education and KOSEF (Korea), and CONICET and UBACyT (Argentina).

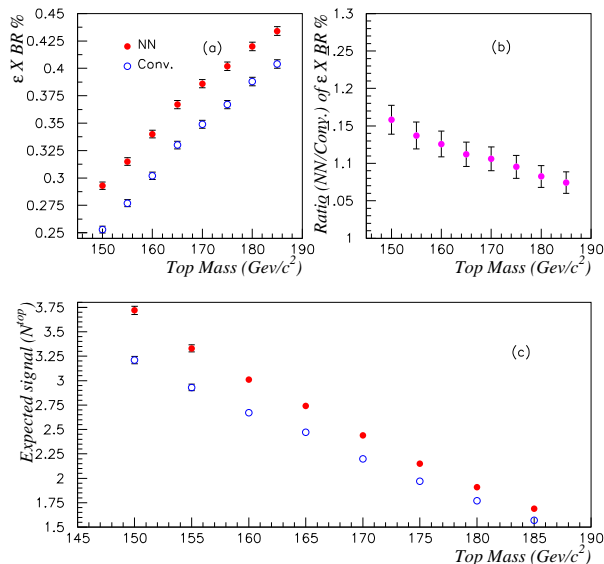


FIG. 12. The neural network analysis compared to the standard analysis, for $D\bar{0}$'s Run 1. (a) Efficiency times branching ratio (%); (b) Ratio of NN analysis efficiency to standard analysis efficiency; (c) Expected number of signal events. Uncertainties displayed are statistical only; the systematic uncertainties (included in Table I) are highly correlated between the two analyses.

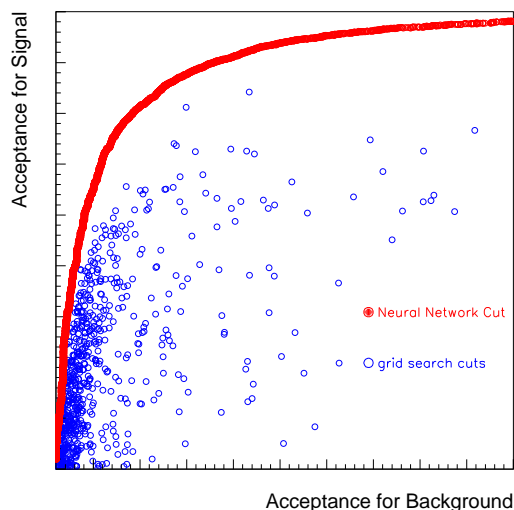


FIG. 13. The neural network analysis compared to the standard analysis. Each point represents a different set of selection requirements.

- [1] CDF Collaboration (F. Abe *et al.*), Phys. Rev. Lett. **74**, 2626 (1995); $D\bar{0}$ Collaboration (S. Abachi *et al.*), Phys. Rev. Lett. **74**, 2632 (1995).
- [2] P. Bhat, H. Prosper, and S. Snyder, Int. J. Mod. Phys. **A13**, 5113 (1998).
- [3] D. E. Rumelhart and J. L. McClelland, *Parallel Distributed Processing, Explorations in the Microstructure of Cognition, Vol 1: Foundations* (MIT Press, Boston, 1986); R. Beale and T. Jackson, *Neural Computing: An Introduction* (Adam Hilger, Bristol, 1990).
- [4] $D\bar{0}$ Collaboration (B. Abbott *et al.*), Phys. Rev. **D60**, 012001 (1999); *ibid*, Report No. Fermilab-Pub-99/008-E (1999), hep-ex/9901023, submitted to Phys. Rev. Lett..
- [5] $D\bar{0}$ Collaboration (B. Abbott *et al.*), Phys. Rev. **D58**, 052001 (1998); $D\bar{0}$ Collaboration (S. Abachi *et al.*), Phys. Rev. Lett. **79**, 1197 (1997).
- [6] K. Hornik, M. Stinchcombe, and H. White, Neural Networks **2**, 359 (1989); K.-I. Funahashi, Neural Networks **2**, 183 (1989).
- [7] L. Dudko, in *Proceedings of the 6th International Workshop on New Computing Techniques In Physics Research (AIHENP99), Crete, Greece* (Elsevier North-Holland, Amsterdam, 1999).
- [8] M. C. Smith and S. Willenbrock, Phys. Rev. **D54**, 6696 (1996); T. Stelzer, Z. Sullivan, and S. Willenbrock, Phys. Rev. **D56**, 5919 (1997); A. P. Heinson, A. S. Belyaev, and E. E. Boos, Phys. Rev. **D56**, 3114 (1997).
- [9] T. Tait and C.-P. Yuan, Report No. MSUHEP-71015, hep-ph/9710372 (1997).
- [10] E. Boos, L. Dudko, and T. Ohl, Report No. INP-MSU 99-4/562 (1999), hep-ph/9903215.

- [11] C. Peterson, T. Rönvaldsson, and L. Lönnblad, *Comp. Phys. Comm.* **81**, 185 (1994).
- [12] DØ Collaboration (S. Abachi *et al.*), *Phys. Rev. Lett.* **79**, 1203 (1997).